

Antisymmetry in the quantum Monte Carlo method with the A -function technique: $\text{H}_2 b^3\Sigma_u^+$, $\text{H}_2 c^3\Pi_u$, $\text{He } 1^3S$

R. Bianchi, D. Bressanini, P. Cremaschi, and G. Morosi

Dipartimento di Chimica Fisica ed Elettrochimica and Centro CNR per lo Studio delle Relazioni tra Struttura e Reattività Chimica, Via Golgi 19, 20133 Milano, Italy

(Received 21 October 1992; accepted 26 January 1993)

The diffusion Monte Carlo method for the solution of the Schrödinger equation for atomic and molecular systems is extended to incorporate the antisymmetry constraint. The sign problem is treated constraining the diffusion process of signed walkers within the fluctuating nodes of a function A , defined as sum of Gaussians centered on the psips. The function A is able to build up the full nodal surface in the $3N$ dimensional space. The algorithm is shown to scale as $N_\alpha^3 + N_\beta^3$ where N_α and N_β are the number of α and β electrons. Results are given for the $b^3\Sigma_u^+$ and $c^3\Pi_u$ states of H_2 and the 1^3S state of He.

I. INTRODUCTION

The diffusion quantum Monte Carlo (DMC) method is emerging as an alternative to the *ab initio* methods for solving the Schrödinger equation.

The formal similarity between the Schrödinger equation in imaginary time and a generalized diffusion equation implies that the wave function is interpreted as a concentration, i.e., a quantity everywhere positive. This interpretation does not represent a constraint for the simulation process as long as one is dealing with the ground state of boson systems which are described by non negative wave functions, but it does create difficulties in the description of fermion systems where, due to the antisymmetry, positive and negative regions are present in the wave function domain.

Since the Schrödinger equation, by itself, allows both symmetric and antisymmetric solutions, the antisymmetry must be handled with some kind of external constraint, such as the determinantal representation of the wave function normally used in the analytical methods.

Anderson¹ introduced the antisymmetry in the QMC simulation using the fixed-node method which is based on an *a priori* knowledge of approximate nodal surfaces. Since this technique gives an upper bound to the true energy when the fixed nodal surfaces are not the exact ones, a method for node relaxation has been devised,² but, since the wave function for the fermion ground state is obtained as a difference between two boson distributions, its applicability is severely limited by numerical instability.

Both methods are encompassed by the mirror potential method by Carlson and Kalos:³ A repulsive potential generated by the walkers of opposite sign prevents the psip to penetrate regions of different sign. The fixed node approximation corresponds to an infinite repulsive potential, while the node release method corresponds to zero potential.

A way to stabilize two signed distributions, for low dimensional systems, was devised by Arnow *et al.*:⁴ They introduced the crucial idea of cancellation of psips with different sign through a composite Green's function.

Alternative DMC techniques based on the cancellation

of pairs of psips of opposite sign in close proximity were introduced by Coker and Watts⁵ and by Elser.⁶ These methods implement the antisymmetry principle, $\Psi(\mathbf{r}_1, \mathbf{r}_2) = -\Psi(\mathbf{r}_2, \mathbf{r}_1) = 0$ when $\mathbf{r}_1 = \mathbf{r}_2$, in a loose way, adopting a proximity criterion as it is practically impossible to find two walkers in exactly the same position. These methods define only isolated zeros and not the complete nodal surfaces: In fact, the antisymmetry principle alone cannot define the whole $(3N-1)$ dimensional nodal hypersurface, but only a $(3N-3)$ D subhypersurface^{7,8} because of the simultaneous permutation of the three spatial coordinates of the electrons; the $(3N-1)$ D nodal hypersurface is correctly defined only through the continuity of the wave function. Consequently, when sampling a wave function one should take into account the whole collection of walkers and not only a pair.

This step has been recently undertaken by Anderson *et al.*⁹ and Kalos and Zhang,¹⁰ building on the previous work by Arnow *et al.*⁴ They defined new Green's function methods introducing a conditional probability of diffusion (either directly during the walker movement, or indirectly during the weighting step), which depends on the whole collection of psips, i.e., the propagator is the sum of the propagators of all the walkers.

In a previous letter¹¹ we presented a different algorithm (the A -function technique) which introduces the antisymmetry constraint in the DMC method using only the wave function representation inherent to the simulation process: All psips moving across regions of different sign are deleted. In this paper we present a more complete description of our method and of a closely related algorithm based on the Voronoi tiling of the configuration space.

II. ALGORITHM

The diffusion quantum Monte Carlo method described by Anderson^{1,12,13} is based on the solution of the diffusion equation by a random walk. The diffusion process starts by defining a collection of n random walkers (psips, replicas, or configurations), each one representing a possible geometrical configuration of the quantum system being simulated. The psip density at a given time τ is proportional to

the wave function and the ensemble of the psips is a sample from the exact wave function $\Psi(\mathbf{R},\tau)$, that is the quantum state of the system at time τ is represented by a sum of n Dirac δ functions in the coordinate space

$$\Psi(\mathbf{R},\tau) = \lim_{n \rightarrow \infty} F(\mathbf{R},\tau)$$

with

$$F(\mathbf{R},\tau) = \sum_i^n w_i \delta(\mathbf{R} - \mathbf{R}_i^{(\tau)}), \quad (1)$$

where \mathbf{R} is the coordinate vector of $3N$ dimensions, N being the number of electrons of the system; F represents the ensemble of psips present at time τ , centered at $\mathbf{R}_i^{(\tau)}$ and with positive or negative sign according to the sign of the w_i weights; the absolute value of w_i is equal to the psip multiplicity. The presence of signed configurations defines the nodal surfaces of the wave function in the sense that a concentration of positive (negative) psips defines a positive (negative) region of $\Psi(\mathbf{R})$.

From a computational point of view, the $3N$ dimensional space of the system must be sampled by a large number of psips to converge to the exact energy value.^{14,15} However only an infinite number of walkers defines the sign of $F(\mathbf{R},\tau)$ in every position, allowing to detect a node crossing during the diffusion process and avoiding the collapse of the system to a sum of two independent boson ground states. To overcome these problems each Dirac δ function is approximated by a multidimensional Gaussian;^{5,16} therefore $\Psi(\mathbf{R},\tau)$ is approximated by the new function $A(\mathbf{R},\tau)$ defined as

$$\begin{aligned} \Psi(\mathbf{R},\tau) &\simeq A(\mathbf{R},\tau) \\ &= \sum_i^n w_i \left[g(\mathbf{R}, \mathbf{R}_i^{(\tau)}) + \sum_m^P (-1)^m g(\mathbf{R}, P_m \mathbf{R}_i^{(\tau)}) \right] \\ &= \sum_i^n w_i \mathcal{A} [g(\mathbf{R}, \mathbf{R}_i^{(\tau)})], \end{aligned} \quad (2)$$

$$g(\mathbf{R}, \mathbf{R}_i^{(\tau)}) = \exp[-\alpha(\mathbf{R} - \mathbf{R}_i^{(\tau)})^2], \quad (3)$$

where P is the number of coordinate permutations between electrons with equal spin, P_m is the m th permutation operator, $\mathbf{R}_i^{(\tau)}$ is the $3N$ dimensional position of the i th psip, and \mathbf{R} the position where the function is evaluated, α is the half-width of the Gaussian. The antisymmetrizer \mathcal{A} permutes only electrons with the same spin. Obviously, for n and α tending to infinity the A function is an exact representation of $\Psi(\mathbf{R},\tau)$, apart from a normalization factor.

It is worth noting that $A(\mathbf{R},\tau)$, being antisymmetric and continuous on the $3N$ dimensional space, is zero on a $(3N-1)$ dimensional hypersurface and not only on a $(3N-3)$ D subspace.¹¹ In fact the node equation $\sum_i^n w_i \mathcal{A} [g(\mathbf{R}, \mathbf{R}_i^{(\tau)})] = 0$ is the implicit form of the full nodal surface whose explicit form is consequently defined on the $(3N-1)$ D space.

Because the number of permutations in the A function increases as $N_\alpha! N_\beta!$, this algorithm can apparently be used only for systems with very few electrons. On the other hand, a Gaussian centered on \mathbf{R}_i in the $3N$ dimensional

space can be written as a product of N one-electron Gaussian functions centered on the electrons positions $\mathbf{r}_{1i} \dots \mathbf{r}_{Ni}$ in the 3D space. For $N_\alpha \alpha$ and $N_\beta \beta$ electrons we have

$$\begin{aligned} \mathcal{A} g(\mathbf{R}, \mathbf{R}_i) &= \mathcal{A} [g_1(\mathbf{r}_{1i}, \mathbf{r}_{1i}) g_2(\mathbf{r}_{2i}, \mathbf{r}_{2i}) \dots g_N(\mathbf{r}_{Ni}, \mathbf{r}_{Ni})] \\ &= \det |g_1 g_2 \dots g_{N_\alpha}| \det |g_{N_\alpha+1} g_{N_\alpha+2} \dots g_N|. \end{aligned} \quad (4)$$

Because the numerical evaluation of a determinant of order N scales as N^3 , our algorithm scales as $N_\alpha^3 + N_\beta^3$. This fact is extremely important from the point of view of the feasibility of the algorithm, because methods plagued by an $N!$ factor can be used only for systems with very few electrons.

A more formal derivation of the A function as sum of multidimensional gaussians can be obtained from the integral form of the (imaginary) time dependent Schrödinger equation

$$\Psi(\mathbf{R},\tau) = \int G(\mathbf{R}' \rightarrow \mathbf{R}, \tau) \Psi(\mathbf{R}', 0) d\mathbf{R}', \quad (5)$$

where the Green's function

$$G(\mathbf{R}' \rightarrow \mathbf{R}, \tau) = \langle \mathbf{R} | e^{-\tau H} | \mathbf{R}' \rangle \quad (6)$$

gives the transition probability from \mathbf{R}' to \mathbf{R} in a time τ . According to Eq. (1) in a DMC simulation the wave function at each step can be represented by a sum of weighted delta functions

$$\Psi(\mathbf{R}', 0) \simeq \sum_i w_i \delta(\mathbf{R}' - \mathbf{R}_i). \quad (7)$$

Substituting Eq. (7) into Eq. (5) one obtains

$$\begin{aligned} \Psi(\mathbf{R}, \tau) &\simeq \int G(\mathbf{R}' \rightarrow \mathbf{R}, \tau) \sum_i w_i \delta(\mathbf{R}' - \mathbf{R}_i) d\mathbf{R}' \\ &= \sum_i w_i G(\mathbf{R}_i \rightarrow \mathbf{R}, \tau). \end{aligned} \quad (8)$$

The exact form of the Green's function is usually unknown, but in the short time approximation¹⁷ it is possible to write the evolution operator as

$$\exp(-\tau H) \simeq \exp(-\tau V) \exp(-\tau T) \quad (9)$$

by neglecting the $O(\tau^2)$ terms. Substituting Eq. (9) into Eq. (6) and performing the integration, one obtains the free particle Green's function, times the potential term

$$G(\mathbf{R}_i \rightarrow \mathbf{R}, \tau) = (2\pi\tau)^{-3N/2} e^{-\tau V(\mathbf{R})} e^{-(\mathbf{R} - \mathbf{R}_i)^2 / 2\tau}. \quad (10)$$

The substitution of Eq. (10) into Eq. (8) gives the final Gaussian representation of Ψ

$$\Psi(\mathbf{R}, \tau) \simeq (2\pi\tau)^{-3N/2} e^{-\tau V(\mathbf{R})} \sum_i w_i e^{-(\mathbf{R} - \mathbf{R}_i)^2 / 2\tau}. \quad (11)$$

Equation (11) is equivalent to Eq. (2) if the potential term is interpreted (as it is usually done in the DMC algorithm) as a psip multiplicity and if α is set equal to $1/2\tau$. If τ is identified with the random walk time step, the formal definition of $\alpha = 1/2\tau$ should avoid the parametrization of the problem. In practice this is impossible with only a few thousand psips: For τ in the usual range of 10^{-2} – 10^{-3}

hartree⁻¹ the resulting Gaussian functions would become too narrow, leading to a noninteracting ensemble unable to force the antisymmetry constraint and with completely ill-defined positive and negative regions owing to numerical errors in the inter-Gaussian regions. Only an ensemble size 2 or 3 orders of magnitude larger would allow to use such a narrow width. A value of α greater than $1/2\tau$ simulates the effect of increasing the ensemble size at no cost. Problems of numerical inaccuracy are also found when the Gaussian exponent is too small: The value of the A function at point \mathbf{R} is given by a sum of positive and negative terms with almost identical absolute values. The exponential components of the A function make the acceptable numerical range for α rather narrow and preliminary calculations indicated that its optimal value lies in the $0.1 < \alpha < 1$ range.¹⁸ In conclusion, to avoid numerical errors in the evaluation of the A function, the α value must depend on the number of psips in such a way that the configuration space is significantly filled. As $n \rightarrow \infty$, α must go to infinity in agreement with its correspondence to $1/2\tau$, because an infinite number of psips allows the time step to go to zero, avoiding in this way the short time approximation. In fact, a finite value of τ is required for sampling the configuration space with a finite number of walkers.

While the A function is able to define the statistically correct nodal surfaces (i.e., the signs of the different regions), it does not predict the values of the exact wave function: A spikelike form, reflecting the structure of the discrete psip distribution, is always present but in the limit of an infinite number of psips. However, as our algorithm needs only the sign of the A function, not its absolute value, the lack of this information is not detrimental to our technique.

The nodal surfaces of the A function used in the diffusion process act as an infinite potential absorbing all crossing psips. The simulation of the Schrödinger equation starts at time τ_0 with a set of positive and negative psips obtained either by sampling a known trial wave function or by a fixed node simulation. A random set of signed psips could also be used,¹⁸ but this choice slows down the equilibration process. The psips of the sample S_0 are moved according to the usual random walk to generate a new sample S_1 at time τ_1 . For each i th psip of sample S_1 the value of $A(\mathbf{R}, \tau_0)$ at $\mathbf{R} = \mathbf{R}_i^{(\tau_1)}$ is computed. If this value and the psip have the same sign the configuration is kept, otherwise it is cancelled because a node of the A function was crossed. When this cancellation process is completed, the remaining psips are multiplied or destroyed as usual according to the potential term,¹² generating a new set S'_1 which defines a new $A(\mathbf{R}, \tau_1)$. This procedure is restarted for S'_1 evolving to S_2 at time τ_2 and carried out.

Since the evaluation of the A function is extremely costly, we have devised, but still not thoroughly tested, two possible techniques to speed up the calculations. In the first one, only a subset, randomly extracted from the original set, is used for the A function definition. In the second method, the A function is evaluated at position \mathbf{R} only when the value of a trial function at \mathbf{R} is smaller than a predefined threshold; this technique implicitly assumes

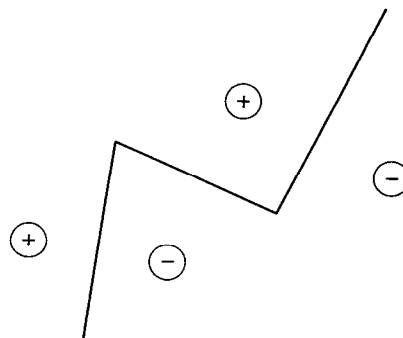


FIG. 1. Voronoi nodes for a model system in two dimensional space.

that the trial wave function nodes are only slightly different from the exact ones. The evaluation of this trial function does not put any extra burden on the simulation because these values are already required by the mixed estimator of the energy.

Since Eq. (9) (the short time approximation) becomes exact only in the limit of $\tau \rightarrow 0$, which implies $\alpha \rightarrow \infty$, it is interesting to investigate which kind of algorithm would correspond to this limit. If in Eq. (2) α tends to infinity, all terms in the sum decay to zero and the one with minimum $\|\mathbf{R} - P_j \mathbf{R}_j\|$ dominates. In other words, in this limit the asymptotic sign of $A(\mathbf{R}, \tau)$ is the sign of the nearest psip (including also all the permutations). In this way the $3N$ dimensional space is tiled with signed Voronoi polyhedra:¹⁹ the Voronoi polyhedron associated with a psip is the minimal polyhedron whose planar faces are defined to be planes which bisect at right angles the lines joining the psip to its neighbors. The set of all the edges between polyhedra with different signs defines the Voronoi nodes. These nodes, as shown in Fig. 1, are not a smooth surface like the ones defined by the A function. This algorithm formally uses δ functions for the $A(\mathbf{R}, \tau)$ representation and the corresponding Voronoi nodes become smooth and approach the nodes of the exact wave function as the number of psips tends to infinity.

The use of the nodes of the Voronoi tiling is computationally faster than that of the full A function: it only requires to compute distances and to select the shortest one, instead of evaluating a sum of exponentials of distances. However, a larger number of psips is required for a good instantaneous description of the nodal surfaces: a small number of psips necessarily requires the use of Gaussians of finite width to give a correct instantaneous description of the nodal structure.¹⁸

It is worth noting that the search of the minimum of $\|\mathbf{R} - P_j \mathbf{R}_j\|$ can be done quite efficiently using an algorithm that solves the "assignment problem" of optimization theory.²⁰ We checked that this algorithm scales as N^3 , at least for $N < 100$, and so the Voronoi algorithm retains the same scaling property of the general A function algorithm.

III. CALCULATIONS

To test the validity of the A -function technique with a broader spectrum of cases than in our previous letter¹¹ and

TABLE I. Simulations using the A function. Energy values in hartree.

System	$E(\text{exact})$	No. of psips	$E(\text{calc.})$
$\text{H}_2 b^3\Sigma_u^+$	-0.7841	1000	-0.7827 \pm 0.0009
		3000	-0.7841 \pm 0.0007
$\text{H}_2 c^3\Pi_u$	-0.7378	1000	-0.7389 \pm 0.0014
		1000	-2.1737 \pm 0.0014

to show its capability to deal with excited states of different symmetry, the $b^3\Sigma_u^+$ and the $c^3\Pi_u$ triplet states of the hydrogen molecule and the 1^3S state of the helium atom have been calculated.

The energy of the systems has been computed using the mixed estimator^{4,21}

$$\langle E \rangle = \int \psi H \psi_T d\mathbf{r} / \int \psi \psi_T d\mathbf{r} \approx \sum_i (H\psi_T)_i / \sum_i (\psi_T)_i, \quad (12)$$

where ψ_T is a trial wave function; this estimator gives a smaller error (Table I) and a faster convergence than those obtained with the average potential technique previously used.¹¹

No guiding function was used in the simulation because we did not want, in any way, to influence the building of the correct nodal structure and the convergence to the desired state. On the other hand, the use of the A function to define the nodes neither prevents, nor makes unnecessary the use of an importance sampling technique to speed up the calculations and reduce the variance.

A fixed time step of 0.001 hartree⁻¹ has been used in all calculations because it introduces a bias small enough to let us be confident about the meaningfulness of our results even without extrapolation to $\Delta\tau=0$. The standard deviation was evaluated using blocks 1000 steps long; the residual correlation between blocks was eliminated by the blocking method.²²

As already pointed out by Anderson *et al.*⁹ in the implementation of their method, we found useful to take advantage of the space symmetry of the state under investigation by including in the construction of the A function the psips generated by the symmetry operators belonging to the point group of the system. If a state has a given symmetry, it is possible to generate from a psip $\mathbf{R} \equiv \{\mathbf{r}_1, \mathbf{r}_2, \dots, \mathbf{r}_N\}$ with sign s the psip $\mathcal{O}\mathbf{R}$ with sign λs , where \mathcal{O} is a symmetry operator of the simulated state and $\lambda = \pm 1$ its character. For example, during the simulation of the $b^3\Sigma_u^+$ state of H_2 , for each psip a replica, generated applying the symmetry plane perpendicular to the internuclear axis, was included in the A function with opposite sign.

The use of the space symmetry operators, in addition to the antisymmetry operator, helps building the correct nodal structure by imposing extra constraints on the position of the nodes of the A function. From this point of view, it was found more useful to include in $A(\mathbf{R}, \tau)$ more psips generated with a symmetry operator than to deal with the same amount of independent walkers.

To monitor a possible collapse to the boson state, during the simulation the overlap between the trial function ψ_T and the exact wave function ψ was computed

$$\int \psi(\mathbf{R}, \tau) \psi_T(\mathbf{R}) d\mathbf{R} = \frac{1}{N} \sum_i^N \psi_T(R_i). \quad (13)$$

This value should remain almost constant: Large fluctuations or changes of sign indicate instability in the convergence to the desired state.

Another possible test is the computation of the number of positive psips in the region where the trial function is negative. This number must remain almost constant if the A -function technique builds up the correct nodes, and small if ψ_T is sufficiently accurate. This test has been used also in preliminary, short simulations to define, for a given number of psips, the α value able to keep apart the positive and negative walker distributions.

A. $\text{H}_2 b^3\Sigma_u^+$

Because the first triplet of the hydrogen molecule is a repulsive state, it was simulated at the arbitrary bond length of 1.4 bohr, for which Kolos and Wolniewicz²³ computed an essentially exact energy of -0.784 15 hartree.

The trial function was a simple determinantal wave function $\psi_T = |\phi_{\sigma g} \phi_{\sigma u}|$, the molecular orbitals being a linear combination of two Slater orbitals with $\xi=0.6$ and 1.3. The corresponding STO-6G calculation gives a variational energy of -0.771 76 hartree.

To simulate the b state and avoid the collapse to the singlet ground state, it is enough to force the antisymmetry constraint on the spatial part of the wave function. However, the symmetry constraints were included in the definition of the A function to obtain a better stabilization of the simulation, as discussed above. For this reason the symmetry plane perpendicular to the nuclear axis was included, a reflection through it changing the sign of the psip.

An exponent of 0.5 was used for the Gaussians in the A function and the simulations were carried out using 1000 and 3000 psips propagated for 200 and 270 blocks, respectively, each one 1000 steps long.

During the simulation process the number of positive psips in the negative region of the trial function fluctuated around 2% \pm 1% of the total number, showing that the A -function technique is able to prevent the collapse to the ground state.

The results reported in Table I show the improvement of the computed energy upon the increase of the number of psips used in the simulation.^{14,15}

B. $\text{H}_2 c^3\Pi_u$

This system was chosen to test the ability of the A -function technique to deal with symmetry constraints, as this state has a different spatial symmetry with respect to the ground triplet state. The simulation was performed at the equilibrium distance of 1.9608 bohr, the corresponding exact energy being -0.737 80 hartree.²⁴ A wave function of the form $\psi_T = |\phi_{\sigma} \phi_{\pi}|$ was adopted for the mixed esti-

mator, the orbitals being linear combinations of a $1s$ Slater orbital with $\zeta=1.24$ and a set of $2p$ with $\zeta=0.6$. The corresponding STO-6G wave function gives a variational energy of -0.72252 hartree.

To avoid the collapse to the energetically more stable Σ state, the psips that generate a sample of π symmetry must be added to those required for getting an antisymmetric A function. For each walker a replica with opposite sign and reflected through the yz plane (z being the internuclear axis) was included.

A Gaussian exponent of 0.5 was used in a simulation with 1000 psips carried on for 200 blocks, each 1000 steps long.

The number of positive psips in the negative region of ψ_T fluctuated around $4\% \pm 1\%$ indicating a stable simulation. The fact that this number is twice the one found in the simulation of $b^3\Sigma_u^+$ might suggest that the trial function used for the b triplet gives a better description of the exact nodes than the one used for the $c^3\Pi_u$ state.

The computed energy, reported in Table I, is in good agreement with the exact value and, once more, gives a clear indication that the A -function technique is able to cope with the problem of the antisymmetry and of the spatial symmetry.

C. He 1^3S

The first triplet state of the helium atom is one of the few cases of polyelectronic systems for which the exact nodes of the wave function are known, so it is often used as a test of QMC methods. Since it is an S state, its wave function depends only on r_1 , r_2 and r_{12} , where r_1 , r_2 are the distances of the two electrons from the nucleus and r_{12} is the interelectronic distance.²⁵ Being the spatial part of the wave function antisymmetric, we can write

$${}^3\psi(r_1, r_2, r_{12}) = -{}^3\psi(r_2, r_1, r_{12})$$

and this means that the exact node is defined by $r_1=r_2$. We used a simple trial wavefunction of the form

$$\psi_T = \exp(-\zeta_1 r_1 - \zeta_2 r_2) - \exp(-\zeta_1 r_2 - \zeta_2 r_1)$$

with $\zeta_1=0.321007$ and $\zeta_2=1.968630$.²⁶ Even if ψ_T is a crude approximation of the exact wave function (the variational energy is -2.16065 hartree with respect to the exact value of -2.1752), it has the correct nodal structure.

Only the psips needed to satisfy the antisymmetry constraint were added to the ensemble used to build the A function during the random walk, while no symmetry constraint was implemented in the simulation.

We found this system more difficult to simulate in comparison with the two H_2 excited states. The reasons could be the higher nuclear charge and the higher correlation since the two electrons in the helium atom are closer than in H_2 ; moreover the hydrogen molecule calculations were facilitated by the use of the symmetry in the A function which reduced the number of degrees of freedom in the construction of the nodal surface. Simulations with 1000 psips, in spite of the variation of the Gaussian expo-

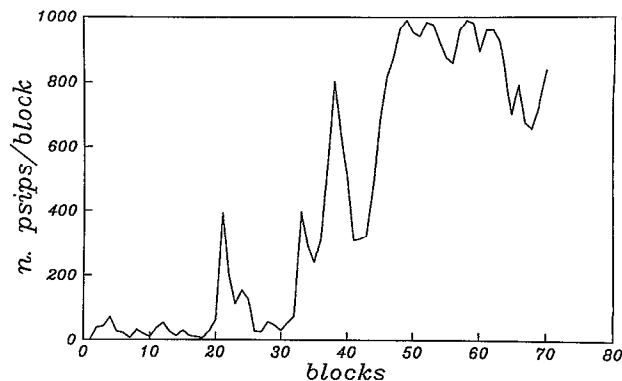


FIG. 2. He 1^3S : flipping of the psips ensemble between regions of opposite sign as evidenced by the increase of the number of positive psips in the negative region of the trial function.

nent and of the time step, were found unstable, not for a collapse to the ground state, but rather for a flipping of the psip ensemble between regions of opposite sign. This effect is evident in Figs. 2 and 3 where the number of positive psips in the negative nodal region and the overlap between ψ and ψ_T [see Eq. (13)] as a function of the number of blocks are reported. Starting at about 40 blocks virtually all positive psips moved to the negative region and this is reflected in the change of the sign of the overlap between Ψ and Ψ_T . Even from this undesired flipping situation it appears clearly that our algorithm is able to prevent the collapse to the ground state: This would result in a complete spread of the positive (and negative) psips over the whole positive and negative regions and not in their concentration in only one of them.

The simulation could be stabilized by increasing the number of psips, but a cheaper way to avoid the undesired flipping between nodal volumes is obtained by updating the A function every k time steps. In fact, if the number of walkers is too small and the A function is updated at each step, a psip is unlikely to move enough in a single step to cross a node, so the A function and their nodes tend to

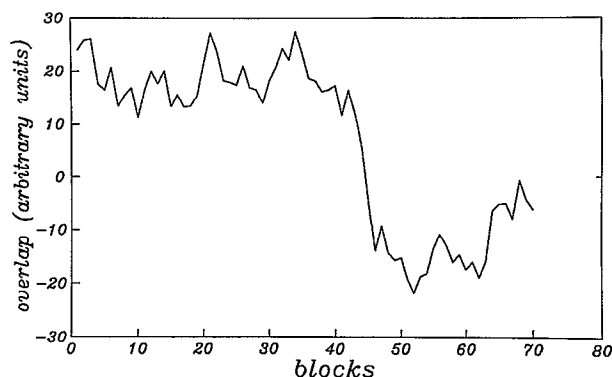


FIG. 3. He 1^3S : flipping of the psips ensemble between regions of opposite sign as evidenced by the change of the sign of the overlap between the exact and the trial wave function [see Eq. (13)].

TABLE II. Simulations using Voronoi nodes. Energy values in hartree.

System	$E(\text{exact})$	No. of psips	$E(\text{calc.})$
$\text{H}_2 \ b^3\Sigma_u^+$	-0.7841	1000 ^a	Collapse
		2000 ^a	-0.7860 ± 0.0005
		1000 × 2 ^{a,b}	-0.7849 ± 0.0005
		1000 × 8 ^{a,c}	-0.7850 ± 0.0005
$\text{He} \ 1^3S$	-2.1752	1000 × 8 ^d	-2.1748 ± 0.0014
		3000 × 8 ^d	-2.1766 ± 0.0012

^aTime step = 0.003 hartree⁻¹.

^bInclusion of the symmetry plane perpendicular to the bond.

^cInclusion of the symmetry plane perpendicular to the bond and of two perpendicular symmetry planes containing the bond.

^dInclusion of the three coordinate planes as symmetry planes.

follow the diffusion process. For the 1^3S state of helium it is sufficient to update the A function every five steps.

The energy of a simulation 400 blocks long, each block 1000 steps long, with 1000 positive psips and $\alpha=0.1$ is reported in Table I. Even if the computed energy is not too good, its value indicates that the A -function technique allows to simulate this triplet state.

D. Voronoi nodes

Several simulations of the first triplet state of H_2 and He have been performed using the nodes obtained with the Voronoi polyhedra technique, as described in Sec. II. The results are reported in Table II.

For both systems this algorithm is unable to keep the positive and negative psips separated if the number of psips is too small and/or the time step too short: The reason is that at each step, for each walker, the closest psip of the previous reference ensemble is very often the same psip which has been moved. In this way a walker will never be killed because it always has, in every position, the same sign of the Voronoi A function. To avoid this problem the time step should be increased or, equivalently, the reference ensemble should be kept unchanged for k steps.

In the H_2 triplet simulation even the increase of the time step to 0.003 hartree⁻¹ and the updating of the reference ensemble every 200 steps were unable to avoid the collapse to the ground state when using 1000 walkers; only the increase of the number of psips or the introduction of symmetric psips in the A function allowed to carry out the simulations (see Table II).

For the helium triplet the calculation with 1000 walkers, updating the reference ensemble every 400 steps, could be completed only with a time step of 0.003 hartree⁻¹; the increase in the number of psips to 3000 and/or the introduction of symmetric psips allowed the use of the standard value of τ in the simulation.

On the whole these results look slightly worse than those obtained by the A -function technique: for the same number of psips the Voronoi algorithm gives an instantaneous approximation of the nodal surfaces worse than the A function.

IV. CONCLUSIONS

In this paper we have presented two algorithms for dealing with the sign problem in quantum Monte Carlo methods. They are exact in the limit of an infinite number of psips and of an infinitesimal time step, like other DMC and GFMC methods. They allow to define a "pure" quantum Monte Carlo method entirely within the stochastic approach.

The results of the calculations of different triplet states of the hydrogen molecule and the helium atom demonstrate the capability of the described algorithms to deal not only with fermion systems, but also with excited states of different symmetry.

The computation of the Voronoi nodes is faster than the implementation of the full A -function technique, but requires a higher number of psips for a correct description of the nodal surfaces.

The potentiality of the A function and the Voronoi techniques for calculations on systems with more than only few electrons is demonstrated by their $(N_\alpha^3 + N_\beta^3)$ scaling.

ACKNOWLEDGMENTS

Partial support of this research by the Progetto Finalizzato "Sistemi informatici e calcolo parallelo" of the Italian CNR is gratefully acknowledged.

- ¹J. B. Anderson, *J. Chem. Phys.* **65**, 4121 (1976).
- ²D. M. Ceperley and B. J. Alder, *Phys. Rev.* **45**, 566 (1980).
- ³J. Carlson and M. H. Kalos, *Phys. Rev. C* **32**, 1735 (1985).
- ⁴D. M. Arnow, M. H. Kalos, M. A. Lee, and K. E. Schmidt, *J. Chem. Phys.* **77**, 5562 (1982).
- ⁵D. F. Coker and R. O. Watts, *Mol. Phys.* **58**, 1113 (1986).
- ⁶V. Elser, *Phys. Rev. A* **34**, 2293 (1986).
- ⁷D. J. Klein and H. M. Pickett, *J. Chem. Phys.* **64**, 4811 (1976).
- ⁸M. Caffarel and P. Claverie, *J. Chem. Phys.* **88**, 1088 (1988).
- ⁹J. B. Anderson, C. A. Traynor, and B. M. Boghosian, *J. Chem. Phys.* **95**, 7418 (1991).
- ¹⁰S. Zhang and M. H. Kalos, *Phys. Rev. Lett.* **67**, 3074 (1991).
- ¹¹R. Bianchi, D. Bressanini, P. Cremaschi, and G. Morosi, *Chem. Phys. Lett.* **184**, 343 (1991).
- ¹²J. B. Anderson, *J. Chem. Phys.* **63**, 1499 (1975).
- ¹³J. B. Anderson, *Int. J. Quantum Chem.* **15**, 109 (1979).
- ¹⁴R. Bianchi, P. Cremaschi, G. Morosi, and C. Puppi, *Chem. Phys. Lett.* **86**, 148 (1988).
- ¹⁵J. H. Hetherington, *Phys. Rev. A* **30**, 2713 (1984).
- ¹⁶M. A. Suhm and R. O. Watts, *Phys. Rep.* **204**, 293 (1991).
- ¹⁷L. S. Schulman, *Techniques and Applications of Path Integration* (Wiley, New York, 1981).
- ¹⁸R. Bianchi, D. Bressanini, P. Cremaschi, and G. Morosi, *Comp. Phys. Commun.* **74**, 153 (1993).
- ¹⁹G. Voronoi and J. Reine, *U. Angew. Math.* **134**, 199 (1908).
- ²⁰R. E. Burkhard and U. Derigs, in *Lecture Notes in Economics and Mathematical Systems*, edited by M. Beckmann, H. P. Kunzi (Springer, Berlin, 1980), Vol. 184.
- ²¹M. A. Lee, K. E. Schmidt, and M. H. Kalos, *Phys. Rev. Lett.* **46**, 728 (1981).
- ²²H. Flyvbjerg and H. G. Petersen, *J. Chem. Phys.* **91**, 461 (1989).
- ²³W. Kolos and L. Wolniewicz, *J. Chem. Phys.* **43**, 2429 (1965).
- ²⁴K. P. Huber and G. Herzberg, *Constants of Diatomic Molecules* (Van Nostrand Reinhold, New York, 1979).
- ²⁵E. H. Hylleraas, *Adv. Quantum Chem.* **1**, 1 (1964).
- ²⁶T. Koga, K. Ohta, and A. Thakkar, *Phys. Rev. A* **37**, 1411 (1988).
- ²⁷C. L. Pekeris, *Phys. Rev.* **115**, 1216 (1959).